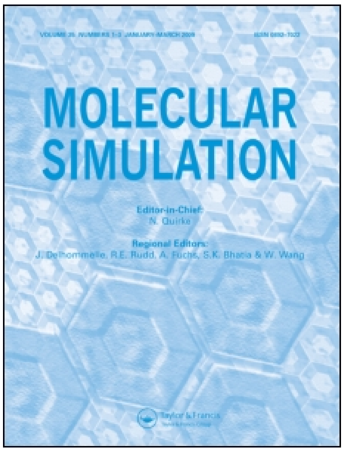

Molecular Simulation
Publication details, including instructions for authors and subscription information:
http://www.informaworld.com/smpp/title~content=t713644482

Accurate determination of normal stress differences via transient-time correlation function - non-equilibrium molecular dynamics (TTCF-NEMD) simulations

Caroline Desgranges[a]; Jerome Delhommelle[a]
[a] Department of Chemistry, University of North Dakota, Grand Forks, ND, USA

To cite this Article Desgranges, Caroline and Delhommelle, Jerome(2009) 'Accurate determination of normal stress differences via transient-time correlation function - non-equilibrium molecular dynamics (TTCF-NEMD) simulations', Molecular Simulation, 35: 5, 405 — 408

To link to this Article: DOI: 10.1080/08927020802575598

URL: http://dx.doi.org/10.1080/08927020802575598

Molecular Simulation
Vol. 35, No. 5, April 2009, 405–408

Accurate determination of normal stress differences via transient-time correlation function – non-equilibrium molecular dynamics (TTCF–NEMD) simulations

Caroline Desgranges and Jerome Delhommelle*

Department of Chemistry, University of North Dakota, Grand Forks, ND, USA

(*Received 17 September 2008; final version received 21 October 2008*)

When a non-Newtonian liquid undergoes shear flow, differences between the values taken by the diagonal elements of the pressure tensor arise. These differences, known as normal stress differences, are notoriously difficult to compute accurately. In this work, we propose to apply the transient-time correlation function (TTCF) formalism together with non-equilibrium molecular dynamics (NEMD) simulations to determine normal stress differences, as well as the corresponding normal stress coefficients, in an atomic fluid undergoing shear flow. Our results shed light on the dependence of normal stress differences and coefficients on the applied shear.

Keywords: normal stress differences; rheology; non-equilibrium molecular dynamics; transient-time correlation function formalism

1. Introduction

The viscosity of a Newtonian liquid undergoing shear flow remains constant for all values of the applied shear rate. Similarly, the three-diagonal elements of the pressure tensor also remain equal to each other (and equal to the pressure at equilibrium) for all shear rates. On the other hand, for a non-Newtonian liquid undergoing shear flow, the viscosity depends on the applied shear rate and differences arise between the diagonal elements of the pressure tensor. These differences are known as normal stress differences and give rise to a wide variety of rheological effects, such as the Weissenberg effect [1]. As noted by Evans and Morriss [2], the normal stress differences, and, as a result, the related normal stress coefficients [3], are very difficult to compute accurately in the course of conventional non-equilibrium molecular dynamics (NEMD) simulations. Few studies have therefore attempted to determine the shear-rate dependence of these differences and results were only reported for extremely high shear rates, i.e. of the order of $10^{11}\,\mathrm{s}^{-1}$ [2,4]. In conventional NEMD simulations, properties are averaged over the steady state. For weak fields, the signal-to-noise ratio is very small and the steady-state response is very noisy. In this case, one cannot extract a reliable estimate for a transport coefficient from the steady-state averages.

In this work, we use the transient-time correlation function (TTCF) formalism [5–7] together with NEMD simulations. Applications of this approach have been restricted so far to a few applications such as, e.g. the evaluation of the viscosity of simple fluids [8–11], the calculation of conductivity of molten salts in the presence of an electric field [12] or of model fluids in the presence of a colour field [13,14]. Other applications include simple liquids undergoing elongational flow [15] and the evaluation of the viscosity for various fluids [16,17]. To our knowledge, no attempt has been made so far to apply the TTCF formalism to accurately determine the normal stress differences in a fluid undergoing shear flow. In this work, we demonstrate that the TTCF approach allows us to compute the normal stress differences for a fluid undergoing shear flow for any value of the applied shear rate. The paper is organised as follows. In the next section, we detail the simulation method. We then present how the TTCF formalism is implemented to evaluate the normal stress differences and coefficients. We finally present and discuss the results obtained in this work.

2. Simulation method

According to the TTCF method, we need to evaluate the response of the fluid over a large number of non-equilibrium trajectories. This requires generating many equilibrium configurations during the course of a long equilibrium trajectory, which are then used as starting points for non-equilibrium trajectories. During the non-equilibrium trajectory, the fluid is subjected to a shear rate γ along the x direction. For all trajectories, the temperature of the system is held constant by applying a Gaussian thermostat. The Gaussian thermostat fixes the value of the streaming kinetic energy (i.e. the kinetic energy relative to the flow), and hence, the temperature according to the

---

*Corresponding author. Email: jdelhommelle@chem.und.edu

ISSN 0892-7022 print/ISSN 1029-0435 online

DOI: 10.1080/08927020802575598
http://www.informaworld.com

equipartition principle [2]. We add that the choice of a specific thermostatting method may lead to dramatically different results for non-equilibrium systems [18–23]. However, those issues generally arise at very high shear rates, beyond the range of shear rates studied in this work.

For the equilibrium trajectory, we use the following set of equations of motion:

$$\dot{\vec{r}}_i = \frac{\vec{p}_i}{m}, \quad \dot{\vec{p}}_i = \vec{F}_i - \alpha\vec{p}_i, \quad \alpha = \frac{\sum_{i=1}^{N}\vec{F}_i \cdot \vec{p}_i}{\sum_{i=1}^{N}\vec{p}_i \cdot \vec{p}_i}, \tag{1}$$

where $\vec{r}_i, \vec{p}_i$ and m are the position, momentum and mass of particle i, $\vec{F}_i$ the force exerted on particle i, N the number of particles and α the thermostatting multiplier.

The equations of motion for the non-equilibrium trajectories are the so-called SLLOD equations of motion [2]. They are defined as follows:

$$\begin{gathered}\dot{\vec{r}}_i = \frac{\vec{p}_i}{m} + \gamma y_i \vec{e}_x, \quad \dot{\vec{p}}_i = \vec{F}_i - \gamma p_y \vec{e}_x - \alpha\vec{p}_i \\ \alpha = \frac{\sum_{i=1}^{N}(\vec{F}_i \cdot \vec{p}_i - \gamma p_x p_y)}{\sum_{i=1}^{N}\vec{p}_i \cdot \vec{p}_i},\end{gathered} \tag{2}$$

where $\vec{e}_x$ is a unit vector along the x-axis and γ is the applied shear rate.

We now discuss how we apply the TTCF formalism to determine the normal stress differences. Following the general derivation proposed by Evans and Morriss [2], we may write that the average of any phase space property B at time t is given by

$$\langle B(t)\rangle = \langle B(0)\rangle - \frac{\gamma V}{k_B T}\int_0^t \langle B(s) \cdot P_{xy}(0)\rangle \mathrm{d}s, \tag{3}$$

in which $P_{xy}(0)$ is the value taken by the shear stress at the start of a non-equilibrium trajectory and the brackets indicate an average taken over all non-equilibrium trajectories. We may use this expression to compute each of the diagonal elements of the pressure tensor. If we choose, e.g. $B(t) = P_{xx}(t)$, we obtain the following expression for $\langle P_{xx}(t)\rangle$:

$$\langle P_{xx}(t)\rangle = \langle P_{xx}(0)\rangle - \frac{\gamma V}{k_B T}\int_0^t \big\langle P_{xx}(s) \cdot P_{xy}(0)\big\rangle \mathrm{d}s. \tag{4}$$

We may also use Equation (3) to compute the normal stress differences. If we choose, e.g. $B(t) = P_{yy}(t) - P_{xx}(t)$, by construction, the average equilibrium $\langle (P_{yy} - P_{xx})(0)\rangle = 0$, which leads to the following expression for $\langle (P_{yy} - P_{xx})(t)\rangle$:

$$\big\langle (P_{yy} - P_{xx})(t)\big\rangle = -\frac{\gamma V}{k_B T}\int_0^t \big\langle (P_{yy} - P_{xx})(s) \cdot P_{xy}(0)\big\rangle \mathrm{d}s. \tag{5}$$

This leads to the following expression for the first normal stress coefficient:

$$\begin{aligned}\langle N_1(t)\rangle &= \frac{\big\langle (P_{yy} - P_{xx})(t)\big\rangle}{\gamma} \\ &= -\frac{V}{k_B T}\int_0^t \big\langle (P_{yy} - P_{xx})(s) \cdot P_{xy}(0)\big\rangle \mathrm{d}s.\end{aligned} \tag{6}$$

Similar expressions may be obtained for the second and third normal stress coefficients,

$$\begin{aligned}\langle N_2(t)\rangle &= \frac{\big\langle (P_{yy} - P_{zz})(t)\big\rangle}{\gamma} \\ &= -\frac{V}{k_B T}\int_0^t \big\langle (P_{yy} - P_{zz})(s) \cdot P_{xy}(0)\big\rangle \mathrm{d}s,\end{aligned} \tag{7}$$

$$\begin{aligned}\langle N_3(t)\rangle &= \frac{\langle (P_{xx} - P_{zz})(t)\rangle}{\gamma} \\ &= -\frac{V}{k_B T}\int_0^t \big\langle (P_{xx} - P_{zz})(s) \cdot P_{xy}(0)\big\rangle \mathrm{d}s.\end{aligned} \tag{8}$$

We use the Weeks–Chandler–Anderson modification of the Lennard-Jones potential to model the interactions between particles. If r is the distance between two particles, the interaction energy between particles is given by $\phi(r) = -4\varepsilon\left[(\sigma/r)^6 - (\sigma/r)^{12}\right] + \varepsilon$ for $r \le 2^{1/6}\sigma$ and 0 otherwise. We use the conventional system of reduced units in the rest of this work [24]. In this work, we consider systems of $N = 512$ particles at constant number density ($n = 0.84$) and constant temperature ($T = 0.75$). Using the operator splitting algorithm presented in Ref. [25], we integrate the equations of motion with a time step of 5×10^{-3}. We apply the Lees–Edwards periodic boundary conditions to the system in the three directions of space [24]. The liquid is initially equilibrated for 10^6 time steps. We then carry out a long equilibrium trajectory in order to generate the equilibrium configurations serving as starting points for the non-equilibrium trajectories. We create 80,000 equilibrium configurations at intervals of 10 time units. In order to increase the efficiency of the procedure, we apply three different mapping procedures, i.e. time-reversal mapping [2], mirror symmetry for x and p_x [2] and the combination of the time-reversal mapping and the mirror symmetry [2]. We then perform a cyclic permutation of the coordinates and momenta over the three directions of space. The 960,000 configurations so obtained were the starting points for the non-equilibrium trajectories. These mappings rigorously lead to the same average value of the three-diagonal elements of the pressure tensor.

3. Results and discussion

We show in Figure 1 the results for the diagonal element $\langle P_{xx}(t)\rangle$ of the pressure tensor given in Equation (4) at a high shear rate (0.25) as well as at a much lower value of the applied shear (10^{-3}). The results obtained for the other two-diagonal elements are qualitatively the same and therefore are not shown here. We also plot in Figure 1 the results obtained by evaluating directly the average of $P_{xx}(t)$ over the $N_t = 960,000$ non-equilibrium trajectories according to the following equation:

$$\langle P_{xx}(t)\rangle = \frac{\sum_{i=1}^{N_t} P_{xx,i}(t)}{N_t}. \qquad (9)$$

Figure 1 demonstrates that the TTCF method gives accurate values for the diagonal element for a wide range of applied shear rates. Figure 1 establishes that the TTCF estimate and the direct average are in excellent agreement for both values of the applied shear rate, thereby demonstrating the validity of the TTCF approach.

At large signal-to-noise ratios, or, in other words, at high shear rates, the steady state average of the three-diagonal elements of the pressure tensor is markedly different. For instance, for a shear rate of 1, the steady-state values obtained by calculating the direct average are $\langle P_{xx}\rangle = 7.21 \pm 0.07$, $\langle P_{yy}\rangle = 7.24 \pm 0.06$ and $\langle P_{zz}\rangle = 6.88 \pm 0.06$. As a result, the normal stress differences are larger than the magnitude of the fluctuations observed in Figure 1 for both the direct average and the TTCF estimate and both approaches give reliable estimates for the normal stress differences and coefficients. However, as shown in Figure 1 for the lower value of the shear rate, the magnitude of the fluctuations for the direct average remains the same as that observed at high shear rates. In fact, the fluctuations for the direct average of the diagonal elements of the pressure tensor become considerably larger than those observed for the TTCF estimate. This means that, for a low signal-to-noise ratio, computing a direct average in the steady state of the normal stress differences yields unreliable results. This can be best seen on Figure 2, in which we have plotted the first normal stress coefficient $\langle N_1(t)\rangle$ calculated either as a direct average or with the TTCF approach, as given in Equation (6). Figure 2 clearly shows that the direct average of the first normal stress coefficient exhibits very large fluctuations (from -1 to $+1$) and never really reaches a steady state. On the other hand, the TTCF estimate reaches a plateau in the steady state with a value of $\langle N_1\rangle = 0.025 \pm 0.005$.

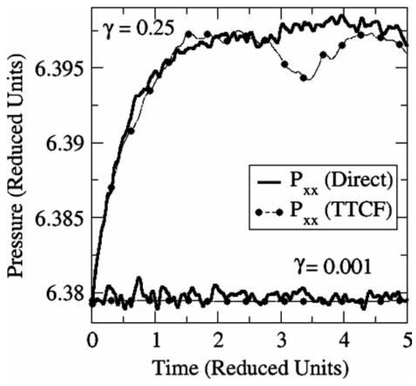

Figure 1. Diagonal element $\langle P_{xx}(t)\rangle$ of the pressure tensor computed according to the TTCF method (Equation (4)) or as a direct average (Equation (9)) for a shear rate of 0.25 (top) and a shear rate of 10^{-3} (bottom).

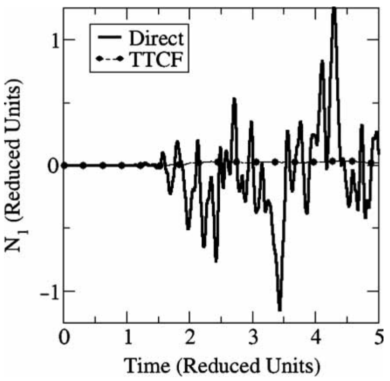

Figure 2. First normal stress coefficient $\langle N_1(t)\rangle$ computed according to the TTCF method (Equation (6)) or as a direct average (Equation (9)) for a shear rate of 10^{-3}.

We show in Figure 3 the results obtained for the three normal stress coefficients. While both the second and third normal stress coefficients steadily increase with the value of the shear rate, the first normal stress coefficient is a non-monotonic function of the shear rate and exhibits a maximum around a shear rate of 0.25. Following Evans and Morriss [2], we fitted power laws of the shear rate to the results obtained for the normal stress coefficients. We obtained the following fits: $\langle N_1(t)\rangle = 0.033\gamma^{-0.57}$,

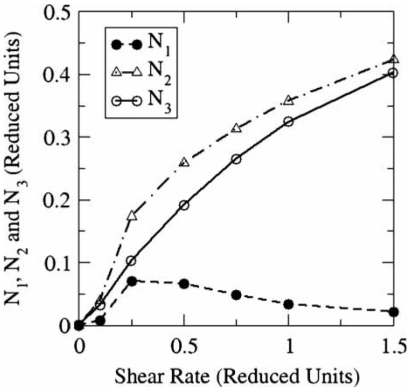

Figure 3. First, second and third normal stress coefficients against the applied shear rate.

$\langle N_2(t)\rangle = 0.354\gamma^{0.45}$, and $\langle N_3(t)\rangle = 0.315\gamma^{0.62}$ with a relative root mean square error of 0.017, 0.004 and 0.006, respectively. Not surprisingly, because of its non-monotonic variation, the first normal stress coefficient is poorly described by a power law. This is consistent with the findings of Evans and Morriss [2]. On the other hand, our results show that the variations of the two other normal stress coefficients are accurately described by a power law.

In this work, we perform TTCF–NEMD simulations to evaluate the normal stress differences and coefficients of a simple fluid undergoing shear flow for any value of the applied shear rate. In particular, we show that the proposed approach clearly outperforms the calculation of direct averages at low shear rates, when the signal-to-noise ratio becomes weak. We give a full account of the dependence of the normal stress differences and coefficients on the applied shear rate. Although the proposed approach is expensive from a computational standpoint, its application to more complex fluids, such as models of polymers, is very promising. For these systems, non-Newtonian effects, such as the onset of normal stress differences, will arise at low shear rates, which make those systems ideally suited to be studied with the TTCF approach.

References

[1] J.C. Rainwater, H.J.M. Hanley, T. Paskiewicz, and Z. Petru, *Non-Newtonian flow of a model liquid between concentric cylinders*, J. Chem. Phys. 83 (1985), pp. 339–347.
[2] D.J. Evans and G.P. Morriss, *Statistical Mechanics of Non-equilibrium Liquids*, Academic Press, London, 1990.
[3] S. Hess, C. Aust, L. Bennett, M. Kroger, C. Pereira Borgmeyer, and T. Weider, *Rheology: from simple to complex fluids*, Physica A 240 (1997), pp. 126–144.
[4] J. Delhommelle and J. Petravic, *Shear viscosity of molten sodium chloride*, J. Chem. Phys. 118 (2003), pp. 2783–2791.
[5] W.M. Visscher, *Transport processes in solids and linear-response theory*, Phys. Rev. A 10 (1974), pp. 2461–2472.
[6] J.W. Dufty and M.J. Lindenfeld, *Non-linear transport in the Boltzmann limit*, J. Stat. Phys. 20 (1979), pp. 259–301.
[7] E.G.D. Cohen, *Kinetic theory of non-equilibrium fluids*, Phys. A 118 (1983), pp. 17–42.
[8] G.P. Morriss and D.J. Evans, *Nonlinear shear viscosity in two dimensions*, Phys. Rev. A 39 (1989), pp. 6335–6345.
[9] I. Borzsak, P.T. Cummings, and D.J. Evans, *Shear viscosity of a simple fluid over a wide range of strain rates*, Mol. Phys. 100 (2002), pp. 2735–2738.
[10] J. Petravic and P. Harrowell, *Linear response theory for thermal conductivity and viscosity in terms of boundary fluctuations*, Phys. Rev. E 71 (2005), 061201.
[11] J. Delhommelle and P.T. Cummings, *Simulation of friction in nanoconfined fluids for an arbitrarily low shear rate*, Phys. Rev. B 72 (2005), 172201.
[12] C. Desgranges and J. Delhommelle, *Molecular simulation of transport in nanopores: Application of the transient-time correlation function formalism*, Phys. Rev. E 77 (2008), 027701.
[13] C. Desgranges and J. Delhommelle, *Estimating the conductivity of a nanoconfined fluid subjected to an experimentally accessible external field*, Mol. Simul. 34 (2008), pp. 177–181.
[14] J. Delhommelle, P.T. Cummings, and J. Petravic, *Conductivity of molten sodium chloride in an arbitrarily weak dc electric field*, J. Chem. Phys. 123 (2005), 114505.
[15] B.D. Todd, *Application of transient-time correlation functions to nonequilibrium molecular-dynamics simulations of elongational flow*, Phys. Rev. E 56 (1997), pp. 6723–6728.
[16] G. Pan and C. McCabe, *Prediction of viscosity for molecular fluids at experimentally accessible shear rates using the transient-time correlation function formalism*, J. Chem. Phys. 125 (2006), 194257.
[17] C. Desgranges and J. Delhommelle, *Shear viscosity of liquid copper at experimentally accessible shear rates: application of the transient-time correlation function formalism*, J. Chem. Phys. 128 (2008), 084506.
[18] J. Delhommelle, J. Petravic, and D.J. Evans, *Reexamination of string phase and shear thickening in simple fluids*, Phys. Rev. E 68 (2003), 031201.
[19] J. Delhommelle, J. Petravic, and D.J. Evans, *On the effects of assuming the flow profile in nonequilibrium simulations*, J. Chem. Phys. 119 (2003), pp. 11005–11010.
[20] J. Delhommelle, *Should "lane formation" occur systematically in driven liquids and colloids?* Phys. Rev. E 71 (2005), 016705.
[21] J. Delhommelle, *Simulations of shear-induced melting in two dimensions*, Phys. Rev. B 69 (2004), 144117.
[22] J. Delhommelle, *Onset of shear-thickening in simple fluids*, Eur. Phys. J. E 15 (2004), pp. 65–69.
[23] J. Delhommelle, J. Petravic, and D.J. Evans, *Non-Newtonian behavior in simple fluids*, J. Chem. Phys. 120 (2004), pp. 6117–6123.
[24] M.P. Allen and D.J. Tildesley, *Computer Simulation of Liquids*, Clarendon, Oxford, 1987.
[25] G. Pan, J.F. Ely, C. McCabe, and D.J. Isbister, *Operator splitting algorithm for isokinetic SLLOD molecular dynamics*, J. Chem. Phys. 122 (2005), 094114.